Multitarget likelihood for Track-Before-Detect applications with amplitude fluctuations

Alexandre Lepoutre, Olivier Rabaste, François Le Gland

Multitarget likelihood for Track-Before-Detect applications with amplitude fluctuations

Alexandre Lepoutre, Olivier Rabaste, and François Le Gland.

Abstract

Track-Before-Detect methods jointly detect and track one or several targets from raw sensor measurements. They often require the computation of the measurement likelihood conditionally to the hidden state that depends on the complex amplitudes of the targets. Since these amplitudes are unknown and fluctuate over time this likelihood must be marginalized over the complex amplitude (*i.e.* phase and modulus). It has been demonstrated in [1] that this marginalization can be done analytically over the phase in the monotarget case. In this article, we first propose to extend the marginalization to the modulus in a monotarget setting, and we show that closed-forms can be obtained for fluctuations of type *Swerling* 1 and 3. Second, we demonstrate that, in a multitarget setting, a closed-form can be obtained for the *Swerling* 1 case. For *Swerling* 0 and 3 models, we propose some approximation to alleviate the computation. Since many articles consider the case of squared modulus measurements, we also consider this specific case in mono and multitarget settings with *Swerling* 0, 1 and 3 fluctuations. Finally, we compare the performance in estimation and detection for the different cases studied and we show the gain, both in detection and estimation, of the complex measurement method over the squared modulus method, for any fluctuation model.

I. Introduction

Filtering consists in recursively finding, at each time step k, the best estimate of an hidden state $\mathbf{X}_k$ from noisy observations. This is a very general problem encountered in many fields such as econometrics, speech recognition and many others [2]. In this article we focus more specifically on the surveillance tracking issue that aims at solving two problems:

- detecting over time the appearance and disappearance of one or several targets in the surveillance area covered by a sensor, for instance a radar, a sonar or an infrared (IR) sensor. This is a detection problem.
- estimating over time as precisely as possible target parameters, for instance position, velocity, bearing and so on, from all the observations provided by the sensor until time step k. This is an estimation problem.

In classic radar processing, the measurement data considered at each time step is a set of detection "hits" obtained by thresholding the raw sensor data after matched filtering. Each "hit" either corresponds to a target or to a false alarm due to clutter or sensor noise. Then, several strategies proposed in the literature can be applied to solve the detection and estimation problem. The MHT (Multiple Hypothesis Tracker) algorithm [3], [4] tries to solve the two problems jointly by considering all possible association hypotheses between hits and tracks. Some other solutions solve the two problems separately: one specific algorithm is devoted to track initiation and termination [5]

while another algorithm performs the tracking itself, assuming that the number of targets is known and solving the hits/tracks association problem if necessary. Among all algorithms proposed to solve this tracking and association problem stands the J/PDAF (Joint/Probability Data Association Filter) algorithms [6], [7].

Whereas these two strategies are different, they share common features. First, the link between the detection "hit" and the target state is often quite simple, so that it is possible to use Kalman or Extended Kalman filter to estimate the target states. Second, both solutions try to solve the association problem that requires to consider all possible associations between "hits" and tracks. When the number of tracks and the number of "hits" are important, the number of possible associations becomes large and often prohibitive to manage. A possible solution to limit the computational cost consists in reducing the number of "hits" by choosing a high detection threshold. However, miss detections will then often occur for low-SNR (Signal to Noise Ratio) targets, making such targets more difficult to track as they will not provide a detection "hit" at each iteration. Thus, a trade-off must be done between the reduction of the number of associations and the detection and tracking capabilities of the system for low-SNR targets.

To overcome these limitations, a different strategy, known as Track-Before-Detect (TBD, has been proposed in the past fifteen years [8], [9], [10]. Contrary to classic techniques that work on detection "hits", TBD methods directly work on raw sensor data. This allows preserving all the information provided by the data and managing jointly target detection and tracking. As all the available information is kept, one can expect detecting and tracking low SNR targets. Nevertheless, the nature of the measurement data is totally different from classic methods. Indeed, considering data after reception processing and matched filtering, the raw sensor measurement consists of a large multidimensional array where each cell value is provided by the corresponding matched filter output. Thus, two problems arise. The first issue is the nature of the measurement. Indeed the highly non-linear link between the observation and the hidden state as well as the large size of the data array do not allow to use techniques based on Kalman Filter. Therefore, the Bayesian filter cannot be solved exactly and one must resort to some approximation. Popular solutions are particle filters [11], [12] and grid-based methods [1]. Particle filter techniques were first developed for TBD applications in the mono-target case in [8] and in the multi-target case in [9], [10]. The second issue is the computation of the measurement likelihood conditionally to the hidden state. In radar applications considered in this article, the measurement equation depends on the complex amplitudes of the targets which are temporally incoherent, *i.e.* they may fluctuate independently from measurement to measurement. The amplitude fluctuation is modelled by a uniform distribution for the phase and a *Swerling* model for the modulus [13]. Note that in another specific framework such as optics, the signal would be real and only the magnitude of the target would be considered. Because of the temporal fluctuation, no information can be gathered over time to estimate the amplitude sequentially contrary to other state parameters. Thus, it is not relevant to compute the likelihood conditionally to these parameters and techniques must be found to compute the likelihood without their knowledge.

The objective of this article is therefore to compute the measurement likelihood in a general multitarget TBD context with unknown fluctuating amplitude parameters. Several solutions have been provided in the literature, mainly in a monotarget setting. The first solution that deals with the unknown complex amplitude considers a

mono-target setting and consists in working on the squared modulus of the complex signal [10], [8], [12], [14], [15]. For such a radical solution that completely discards the phase dependency, two strategies can be considered to deal with the modulus fluctuation. The first one consists in marginalizing the whole likelihood with respect to the density of the modulus fluctuation [15]. In practice, this leads to intractable integrals that must be approximated numerically. The second strategy consists in marginalizing independently the likelihood in each cell [14]. The advantage of this heuristic second solution is that a closed form can be obtained for fluctuations of type *Swerling* 0, 1 and 3 [16]. On the other hand the spatial coherence of the modulus, *i.e.* the fact that the modulus of the target amplitude takes the same value in all cells, is then lost, inducing a possible degradation of performance. Note also that the spatial coherence of the phase is lost for both strategies. This loss was shown in [1] to severely degrade the performance.

To avoid this last drawback, Davey *et al.* [1] have proposed a new strategy that allows preserving the spatial coherence of the phase. Their solution consists in directly working on complex measurement and marginalizing the complex likelihood of the whole data over the phase. It provides better performance than solutions based on squared modulus. However, they mainly investigated the case where the modulus does not fluctuate (*i.e. Swerling* 0 case); for modulus fluctuations, they only provide a general marginalization formula. One of the contributions of this article is an extension of their work with complex measurements to fluctuations of type *Swerling* 1 and 3; we show that closed-forms can be obtained for the monotarget likelihood in both cases.

Furthermore, all the previously discussed strategies with squared modulus or complex measurements were proposed in a monotarget setting. In fact, to our knowledge, the multitarget case has not been investigated in the literature, except for the *Swerling* 1 case with squared modulus of the measurement [10]. Thus, another contribution of this article consists in considering the multitarget case both with squared modulus and complex measurements. In the complex measurement case, we provide a closed-form expression for the likelihood in the *Swerling* 1 case, and we propose in the other fluctuation cases some approximations to alleviate the computational cost. In the squared modulus case, we show that, as soon as at least two targets are present, all phase dependencies cannot be removed from the likelihood; in fact taking the squared modulus permits to remove only one phase, so that other phases must be marginalized. In that latter case, we also propose some approximations in order to reduce the computational complexity.

Overall, this paper intends to provide a generic framework for computing the measurement likelihood in TBD applications in the presence of multiple targets presenting *Swerling* amplitude fluctuations of type 0, 1 and 3. Both complex and squared modulus measurements are considered. Closed-form expressions are provided whenever they are obtainable, and approximations are proposed otherwise. We believe that this article thus represents an exhaustive overview for the computation of the measurement likelihood in TBD, summarized in Table IV that provides the likelihood equation depending on the specific case under consideration, *i.e.* the *Swerling* fluctuation, the measurement type (complex or squared modulus) and the number of targets. This table gathers results from the literature as well as results stated in this article.

This paper is organized as follows. In section II we present the state and measurement models. Then in section III we present solutions for the likelihood computation from complex and squared modulus measurements. In section IV we derive, when possible, closed forms for the likelihood with *Swerling* fluctuations of type 0, 1 and 3 in the monotarget and multitarget cases; when not possible, we propose approximations to alleviate the computational time. Finally in section V we present simulation results that show the gain both in detection and in estimation of the complex measurement method over the squared modulus method.

II. Problem Formulation

In this section we present the framework for tracking multiple targets from complex measurements in a Track-Before-Detect context.

A. Multi-target tracking

Let us denote by $\mathbf{X}_k$ the multitarget state at a given time step k. Assuming that N_k targets are present at this time step k, $\mathbf{X}_k$ can be decomposed as $\mathbf{X}_k = \left[\mathbf{x}_{k,1}^T, \ldots, \mathbf{x}_{k,N_k}^T\right]^T$, where $\mathbf{x}_{k,i}$, with $i \in \{1, \ldots, N_k\}$, represents the individual state of target i at time k, for instance provided by the target position and velocity. Multi-target tracking consists in estimating the multi-target state $\mathbf{X}_k$ and the corresponding number of targets N_k, that may vary over time, from a set of measurements $\mathbf{z}_{1:k}$, where the notation $\mathbf{z}_{1:k}$ represents the set $\{\mathbf{z}_1, \ldots, \mathbf{z}_k\}$. In a Bayesian framework, this estimation is generally performed according to a Minimum Mean Square Error (MMSE) or a Maximum A Posteriori (MAP) criteria, that both require the knowledge of the posterior density $p(\mathbf{X}_k|\mathbf{z}_{1:k})$ of the hidden state $\mathbf{X}_k$ conditionally to the observations $\mathbf{z}_{1:k}$. Using Bayes formula, this posterior density requires in turns the knowledge of the measurement likelihood $p(\mathbf{z}_k|\mathbf{X}_k)$. Computation of $p(\mathbf{z}_k|\mathbf{X}_k)$ in a multitarget TBD context will be the main objective of this paper.

B. Track-Before-Detect Measurement model

In a Track-Before-Detect setting, raw data are directly provided to the tracking filter. Radar raw data for instance consists of range, Doppler and/or 1D or 2D angle measurements. Since matched filtering operations for these parameters are linear, measurements can be considered indifferently before or after matched filtering steps. As the latter approach generally leads to reduced vector sizes and reduced computational cost [17], we will consider here observations after matched filtering along all measurement dimensions. At step k, the measurement $\mathbf{z}_k$ consists of a vector of size N_c corresponding to all measurement cells. It can be expressed by the following non-linear equation that depends on the multi-target state $\mathbf{X}_k$:

$$\mathbf{z}_k = \sum_{i=1}^{N_k} \rho_{k,i} e^{j\varphi_{k,i}} \mathbf{h}(\mathbf{x}_{k,i}) + \mathbf{n}_k, \tag{1}$$

where:

- $\mathbf{h}(\mathbf{x}_{k,i})$ represents the possibly multidimensional ambiguity function of the i^{th} target centered on the target state $\mathbf{x}_{k,i}$. For the sake of simplicity, $\mathbf{h}(\mathbf{x}_{k,i})$ will be denoted $\mathbf{h}_{k,i}$ in the rest of the article.

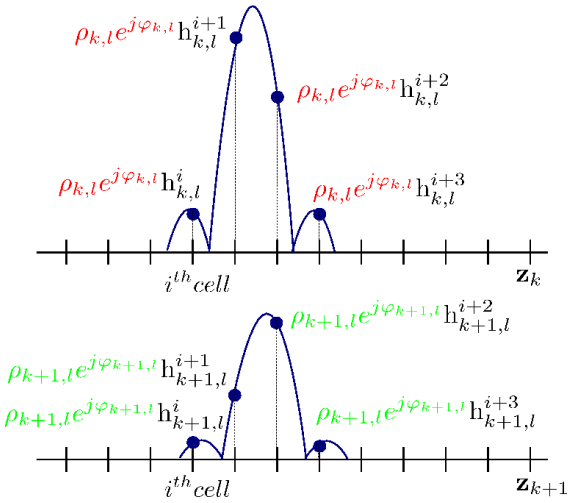

Fig. 1. Received signal (noise-free) corresponding to the l^{th} target at two adjacent time steps k and $k+1$, where dots represent the corresponding measured samples. $\rho_{k,l}$ and $\varphi_{k,l}$ are the same for all cells of $\mathbf{z}_k$ (we denote this feature *spatial coherence*) but their values change independently and randomly over time; there is no *temporal coherence* from step k to step $k+1$.

- $\mathbf{n}_k$ is a zero mean circular complex Gaussian vector with covariance matrix $\mathbf{\Gamma}$.
- $\varphi_{k,i}$ and $\rho_{k,i}$ are respectively the phase and the modulus of the i^{th} target complex amplitude. All variables $\varphi_{k,1:N_k}$ and $\rho_{k,1:N_k}$ are supposed mutually independent, and independent from $\mathbf{n}_k$.

Each phase $\varphi_{k,i}$ is supposed to be unknown and uniformly distributed over the interval $[0, 2\pi)$ at each time step k. Concerning the modulus $\rho_{k,i}$, we consider in this article *Swerling* fluctuations [13] of type 0, 1 and 3, *i.e.* constant modulus for the *Swerling* 0 model, or slow fluctuations for the *Swerling* 1 and 3 models. These models will be detailed in section IV.

An important point to be stressed here is that variables $\rho_{k,1:N_k}$ and $\varphi_{k,1:N_k}$ are *spatially coherent*: this means that the complex target amplitude $\rho_{k,i}e^{j\varphi_{k,j}}$ is identical over all cells where the signal ambiguity function spreads. Taking into account this information can really increase the performance of the Track-Before-Detect algorithms [1]. On the contrary, these variables $\rho_{k,1:N_k}$ and $\varphi_{k,1:N_k}$ are not assumed coherent over time, *i.e.* from time sample k to $k+1$, amplitude parameters fluctuate independently. As a consequence, no information can be gathered over time on these parameters. These dependencies are illustrated in Figure 1.

III. Likelihood computation

A. Likelihood computation with complex measurements

Bayesian Track-Before-Detect algorithms require the computation of the likelihood $p(\mathbf{z}_k \mid \mathbf{X}_k)$, *i.e.* the likelihood of the observation conditionally to the target states. However the measurement equation (1) depends on phase and amplitude parameters $\varphi_{k,1:N_k}$ and $\rho_{k,1:N_k}$ that are unknown and not temporally coherent. Therefore, the expression of the measurement likelihood $p(\mathbf{z}_k \mid \mathbf{X}_k)$ cannot be, in general, directly computed. However it is possible to obtain

the conditional likelihood $p\left(\mathbf{z}_k \mid \mathbf{X}_k, \rho_{k,1:N_k}, \varphi_{k,1:N_k}\right)$ that corresponds to a complex Gaussian density with mean $\boldsymbol{\mu}_k = \sum_{i=1}^{N_k} \rho_{k,i} e^{j\varphi_{k,i}} \mathbf{h}_{k,i}$ and covariance matrix $\boldsymbol{\Gamma}$:

$$p\left(\mathbf{z}_k \mid \mathbf{X}_k, \rho_{k,1:N_k}, \varphi_{k,1:N_k}\right) = \frac{1}{\pi^N \det\left(\boldsymbol{\Gamma}\right)} \exp\left\{-\left(\mathbf{z}_k - \boldsymbol{\mu}_k\right)^H \boldsymbol{\Gamma}^{-1} \left(\mathbf{z}_k - \boldsymbol{\mu}_k\right)\right\}. \tag{2}$$

Then by developing (2) we obtain the following expression:

$$p\left(\mathbf{z}_k \mid \mathbf{X}_k, \rho_{k,1:N_k}, \varphi_{k,1:N_k}\right) = \frac{\exp\left\{-\mathbf{z}_k \boldsymbol{\Gamma}^{-1} \mathbf{z}_k\right\}}{\pi^N \det\left(\boldsymbol{\Gamma}\right)} \times \exp\left\{-\sum_{i=1}^{N_k} \rho_{k,i}^2 \mathbf{h}_{k,i}^H \boldsymbol{\Gamma}^{-1} \mathbf{h}_{k,i} + \sum_{i=1}^{N_k} 2\rho_{k,i} |\mathbf{h}_{k,i}^H \boldsymbol{\Gamma}^{-1} \mathbf{z}_k| \cos\left(\varphi_{k,i} - \xi_{k,i}\right) \right.$$
$$\left. - \sum_{i=1}^{N_k} \sum_{l=i+1}^{N_k} 2\rho_{k,i}\rho_{k,l} \left|\mathbf{h}_{k,i}^H \boldsymbol{\Gamma}^{-1} \mathbf{h}_{k,l}\right| \cos\left(\varphi_{k,i} - \varphi_{k,l} - \phi_{k,il}\right)\right\}, \tag{3}$$

where $\xi_{k,i} = \arg\left(\mathbf{h}_{k,i}^H \boldsymbol{\Gamma}^{-1} \mathbf{z}_k\right)$ and $\phi_{k,il} = \arg\left(\mathbf{h}_{k,i}^H \boldsymbol{\Gamma}^{-1} \mathbf{h}_{k,l}\right)$. Finally the likelihood $p(\mathbf{z}_k \mid \mathbf{X}_k)$ can be obtained by marginalization over parameters $\rho_{k,1:N_k}$ and $\varphi_{k,1:N_k}$:

$$p(\mathbf{z}_k \mid \mathbf{X}_k) = \int \cdots \int_{\mathbb{R}_{\geq 0}^{N_k} \times [0,2\pi)^{N_k}} p\left(\mathbf{z}_k \mid \mathbf{X}_k, \rho_{k,1:N_k}, \varphi_{k,1:N_k}\right) p\left(\varphi_{k,1:N_k}\right) p\left(\rho_{k,1:N_k}\right) d\varphi_{k,1:N_k} d\rho_{k,1:N_k}. \tag{4}$$

First, notice that the spatial coherence is preserved in this formulation thanks to the marginalization. Then, note that the likelihood in Bayesian TBD algorithms such as particle filters can be computed up to a constant, so the constant term

$$\frac{1}{\pi^N \det\left(\boldsymbol{\Gamma}\right)} \exp\left\{-\mathbf{z}_k \boldsymbol{\Gamma}^{-1} \mathbf{z}_k\right\}$$

will be discarded in the rest of the paper, and the computation of the likelihood will be always provided up to this constant.

At last, an important point is that Eq. (4) is often intractable, even for two targets, and must then be computed numerically. We will see in the following that a closed-form can be obtained only for the *Swerling* 1 fluctuations. For other fluctuations type, the numerical implementation implies the evaluation of multiple integrals over several parameters and the computational cost may be rapidly prohibitive in the multitarget case. Fortunately, target contributions can in many cases be separated so that the multitarget likelihood becomes equal to the product of monotarget likelihoods that can be computed in closed-form. This separation can be performed when targets do not interact in the likelihood computation, which can be translated mathematically by the following condition:

$$\left|\mathbf{h}_{k,u}^H \boldsymbol{\Gamma}^{-1} \mathbf{h}_{k,v}\right| \approx 0, \ \forall (u,v), \ u \neq v, \tag{5}$$

that permits to remove all cross terms in Eq.(3). In practice, this hypothesis may arise for instance when $\boldsymbol{\Gamma} = \mathbf{I}_{N_c}$ and targets are far away from each other. Indeed, for each target the ambiguity vector $\mathbf{h}_{k,i}$ has only significant values in a few number of cells around the target location and can be assumed equal to zero elsewhere. Therefore, the scalar product between ambiguity function $\mathbf{h}_{k,u}$ and $\mathbf{h}_{k,v}$ is approximately equal to zero for sufficiently distant targets. Note however that when $\boldsymbol{\Gamma} \neq \mathbf{I}_{N_c}$, condition (5) cannot be verified as straightforwardly and should thus be carefully checked, even for distant targets; in particular the inner product induced by matrix $\boldsymbol{\Gamma}^{-1}$ may mix the target contributions, even when they are located far apart from each other.

Finally under condition (5) the expression of likelihood $p\left(\mathbf{z}_k \mid \mathbf{X}_k, \rho_{k,1:N_k}, \varphi_{k,1:N_k}\right)$ becomes

$$\begin{aligned} p\left(\mathbf{z}_k \mid \mathbf{X}_k, \rho_{k,1:N_k}, \varphi_{k,1:N_k}\right) &\propto \exp\left\{-\sum_{i=1}^{N_k} \rho_{k,i}^2 \mathbf{h}_{k,i}^H \mathbf{\Gamma}^{-1} \mathbf{h}_{k,i} + \sum_{i=1}^{N_k} 2\rho_{k,i} |\mathbf{h}_{k,i}^H \mathbf{\Gamma}^{-1} \mathbf{z}_k| \cos\left(\varphi_{k,i} - \xi_{k,i}\right)\right\} \\ &\propto \prod_{i=1}^{N_k} \exp\left\{-\rho_{k,i}^2 \mathbf{h}_{k,i}^H \mathbf{\Gamma}^{-1} \mathbf{h}_{k,i} + 2\rho_{k,i} |\mathbf{h}_{k,i}^H \mathbf{\Gamma}^{-1} \mathbf{z}_k| \cos\left(\varphi_{k,i} - \xi_{k,i}\right)\right\}, \end{aligned} \tag{6}$$

where the i^{th} term of the product, denoted by

$$\Xi_{\mathbf{z}_k, \mathbf{x}_{k,i}}(\rho_{k,i}, \varphi_{k,i}) = \exp\left\{-\rho_{k,i}^2 \mathbf{h}_{k,i}^H \mathbf{\Gamma}^{-1} \mathbf{h}_{k,i} + 2\rho_{k,i} |\mathbf{h}_{k,i}^H \mathbf{\Gamma}^{-1} \mathbf{z}_k| \cos\left(\varphi_{k,i} - \xi_{k,i}\right)\right\}, \tag{7}$$

only depends on parameters $\rho_{k,i}$ and $\varphi_{k,i}$. As variables $\rho_{k,1:N_k}$ and $\varphi_{k,1:N_k}$ are independent, the joint density (4) then simply becomes

$$p\left(\mathbf{z}_k | \mathbf{X}_k\right) \propto \prod_{i=1}^{N_k} \int_0^{+\infty} \int_0^{2\pi} \Xi_{\mathbf{z}_k, \mathbf{x}_{k,i}}(\rho_{k,i}, \varphi_{k,i}) p(\varphi_{k,i}) p(\rho_{k,i}) d\varphi_{k,i} d\rho_{k,i}. \tag{8}$$

Thus, everything happens as if each target is processed separately. This drastically alleviates the computational complexity of integral (4) and allows processing distant targets with parallel filters or by using the filter developed by Vo *et al.* [18] that made the hypothesis that likelihood can be factorized as in Eq. (8). Of course, when condition (5) is not verified, this simplification can be done only for separated targets, while targets that cannot be separated must be processed by the same filter.

In the monotarget case, integral (4) becomes

$$p\left(\mathbf{z}_k | \mathbf{X}_k\right) \propto \int_0^{+\infty} \int_0^{2\pi} p\left(\mathbf{z}_k | \mathbf{X}_k, \varphi_k, \rho_k\right) p(\varphi_k) p(\rho_k) d\varphi_k d\rho_k. \tag{9}$$

Davey *et al.* [1] have shown in this particular monotarget case that the marginalization can be done over the phase φ_k, providing

$$\begin{aligned} p\left(\mathbf{z}_k \mid \mathbf{X}_k, \rho_k\right) &\propto \int_0^{2\pi} p(\mathbf{z}_k | \mathbf{x}_k, \varphi_k, \rho_k) p(\varphi_k) d\varphi_k, \\ &\propto \exp\left\{-\rho_k^2 \mathbf{h}_k^H \mathbf{\Gamma}^{-1} \mathbf{h}_k\right\} \mathrm{I}_0\left(2\rho_k \left|\mathbf{h}_k^H \mathbf{\Gamma}^{-1} \mathbf{z}_k\right|\right). \end{aligned} \tag{10}$$

Then, the likelihood is obtained by integrating (10) over the density of parameter ρ_k that depends on the fluctuation model considered.

B. Likelihood computation with squared modulus

In the previous section, we have presented the exact computation of the likelihood from complex measurements. In this section, we now expose a different approach often considered in the literature, that consists in working only with the squared modulus of the complex data [14], [15], [10]. This approach is interesting in applications where only the squared modulus of the data is available but also because it permits to remove the phase dependency in a monotarget setting. This simplifies in some extent the computations, at the cost of losing the spatial coherence of the phase. Squared modulus were also considered in an application involving two targets with *Swerling* 1 amplitude fluctuations [10]. In this specific application, the spatial coherence of the target amplitude was not considered,

thus simplifying the computation at the cost of some information loss. We will derive here the general multitarget likelihood in the squared modulus framework. It differs from expressions obtained in the literature since it does not make any approximation and thus properly takes into account the spatial coherence of the complex amplitude. Moreover we show that the squared modulus approach does not permit in the multitarget setting to remove all phase dependencies. Thus, as with complex measurements, these phase variables must be taken into account, for instance by marginalization.

First, let us assume, as in the literature [1], [10], [8], that the covariance matrix is given by $\mathbf{\Gamma} = 2\sigma^2\mathbf{I}_{N_c}$. It means that complex noise samples $\mathbf{n}_k$ are mutually independent. Note however that, since modulus $\rho_{k,1:N_k}$ and phases $\varphi_{k,1:N_k}$ are random variables and spatially coherent at time k, this hypothesis does not allow to establish that signal samples from $\mathbf{z}_k$ are independent; these samples are independent only conditionally to variables $\rho_{k,1:N_k}$ and $\varphi_{k,1:N_k}$. With a slight abuse of notation, we denote by $|\mathbf{z}_k|^2$ the vector of squared modulus of the complex signal : $|\mathbf{z}_k|^2 = [|z_k^1|^2, \ldots, |z_k^{N_c}|^2]^T$. As a consequence, samples from $|\mathbf{z}_k|^2$ are also independent conditionally to variables $\rho_{k,1:N_k}$ and $\varphi_{k,1:N_k}$ and we can write,

$$p(|\mathbf{z}_k|^2 \mid \mathbf{X}_k, \rho_{k,1:N_k}, \varphi_{k,1:N_k}) = \prod_{l=1}^{N_c} p(|z_k^l|^2 \mid \mathbf{X}_k, \rho_{k,1:N_k}, \varphi_{k,1:N_k}). \tag{11}$$

The desired density $p(|\mathbf{z}_k|^2 \mid \mathbf{X}_k)$ can then be obtained from $p(|\mathbf{z}_k|^2 \mid \mathbf{X}_k, \rho_{k,1:N_k}, \varphi_{k,1:N_k})$ exactly in the same way as with complex measurements, by marginalizing over all variables $\rho_{k,1:N_k}$ and $\varphi_{k,1:N_k}$. Remark that the hypothesis of independence is absolutely necessary here to establish Eq.(11). The condition $\mathbf{\Gamma} = 2\sigma^2\mathbf{I}_{N_c}$ can be generalized to diagonal covariance matrices, but the case where $\mathbf{\Gamma}$ is not a diagonal matrix is much more complicated even for two coupled variables: in that case, squared modulus samples are correlated, thus leading to distributions with no closed-form, for instance multivariate Rayleigh distribution in the *Swerling* 1 case [19]. Note also that in practice, this hypothesis is verified with classic matched filtering in presence of white Gaussian noise and an appropriate sampling rate, but it may not be verified anymore when modifying the reception processing, for instance by applying classic weighting windows such as Hamming, Bartlett, Hann, etc. [20]. Before going further into the computation, we would like to highlight here an interesting property that arises when considering squared modulus of complex data, and that has never been discussed to our knowledge in the literature: although N_k targets are present, providing N_k different and independent random phases $\varphi_{k,1:N_k}$, it is possible to show, by changing the set of parameters, that density $p(|z_k^l|^2 \mid \mathbf{X}_k, \rho_{k,1:N_k}, \varphi_{k,1:N_k})$ effectively depends only on $N_k - 1$ phase variables. Indeed the variable $|z_k^l|^2$ can be defined up to an arbitrary phase φ' since $|z_k^l|^2 = |e^{\varphi'} z_k^l|^2$, and we can write for instance

$$\left|z_k^l\right|^2 \quad = \quad \left|\rho_{k,1} h_{k,1}^l + \sum_{i=2}^{N_k} \rho_{k,i} e^{j\varphi'_{k,i}} h_{k,i}^l + {n'}_k^l\right|^2 \tag{12}$$

where all ${n'}_k^l = n_k^l e^{-j\varphi_{k,1}}$ are still independent circular symmetric complex Gaussian noise samples, and phases $\varphi'_{k,i} = \varphi_{k,i} - \varphi_{k,1}$ are still uniform variables distributed over the interval $[0, 2\pi)$. Thus, $|z_k^l|^2$ only depends on $N_k - 1$ phase variables. Therefore, taking the squared modulus of the complex signal leads to drop out the dependence of one and only one phase. As a consequence in a monotarget setting the density of $|z_k^l|^2$ does not depend any longer on

the phase φ_k but only on the modulus; this is one of the main reasons to use such a technique in a TBD monotarget algorithm. On the contrary, in the multitarget setting, taking the squared modulus does not remove all dependencies on the phases! This dependency remains present through coherent summations of the target contributions in each cell. Discarding it may lead to losing all the information provided by the spatial coherence of the phase variables.

Conditionally to variables $\mathbf{X}_k$, $\rho_{k,1:N_k}$ and $\varphi'_{k,2:N_k}$, each sample $\frac{|z_k^l|^2}{\sigma^2}$ follows a non central chi-square distribution with two degrees of freedom; indeed it corresponds to the sum of the square of two non-centered Gaussian variables. The density $p(|z_k^l|^2 \mid \mathbf{X}_k, \rho_{k,1:N_k}, \varphi'_{k,2:N_k})$ is thus given by:

$$p(|z_k^l|^2 \mid \mathbf{X}_k, \rho_{k,1:N_k}, \varphi'_{k,2:N_k}) = \frac{1}{2\sigma^2} \exp\left\{ -\frac{|z_k^l|^2}{2\sigma^2} - \frac{\gamma^l\left(\varphi'_{k,2:N_k}, \rho_{k,1:N_k}\right)}{2} \right\} \mathrm{I}_0\left(\sqrt{\frac{\gamma^l\left(\varphi'_{k,2:N_k}, \rho_{k,1:N_k}\right)|z_k^l|^2}{\sigma^2}} \right), \tag{13}$$

where I_0 is the modified Bessel function of the first kind and $\gamma^l\left(\varphi'_{k,2:N_k}, \rho_{k,1:N_k}\right)$ is the non centrality parameter equal to

$$\gamma^l\left(\varphi'_{k,2:N_k}, \rho_{k,1:N_k}\right) = \frac{\left| \rho_{k,i} h_{k,i}^l + \sum_{i=2}^{N_k} \rho_{k,1} e^{j\varphi'_{k,1}} h_{k,i}^l \right|^2}{\sigma^2}. \tag{14}$$

At this step, mono and multitarget cases are different, and we will consider them separately in the following. Finally, note that, as with complex measurements, the likelihood can be computed up to a constant. Therefore terms $\frac{1}{2\sigma^2} \exp\left\{-\frac{|z_k^l|^2}{2\sigma^2}\right\}$ will be discarded in the rest of the paper.

1) The monotarget case: In a monotarget setting, the non-centrality parameter in each cell becomes

$$\gamma^l\left(\rho_k\right) = \frac{\rho_k^2 |h_k^l|^2}{\sigma^2} \tag{15}$$

and does not depend on φ_k. The joint likelihood can then be obtained by marginalizing Eq.(11) over the parameter ρ_k:

$$p(|\mathbf{z}_k|^2 \mid \mathbf{X}_k) = \int_0^\infty \prod_{l=1}^{N_c} p(|z_k^l|^2 \mid \mathbf{X}_k, \rho_k) p(\rho_k) d\rho_k, \tag{16}$$

where $p(\rho_k)$ is the density for the parameter ρ_k. As for complex measurements, this marginalization allows preserving the spatial coherence of the parameter ρ_k. Since integral (16) is, to our knowledge, intractable for *Swerling* fluctuations models of type 1 and 3 since it consists in integrating N_c Bessel functions, it must be in that case approximated numerically. An heuristic solution was proposed by Rutten *et al.* [14] that consists in assuming that samples $|z_k^1|^2, \ldots, |z_k^{N_c}|^2$ are independent. Recall that this is not true in general because of the spatial coherence of random variable ρ_k. Under this assumption, it comes that

$$p(|\mathbf{z}_k|^2 \mid \mathbf{X}_k) = \prod_{l=1}^{N_c} p(|z_k^l|^2 \mid \mathbf{X}_k), \tag{17}$$

where the likelihood in each cell is obtained by marginalization over ρ_k:

$$p(|z_k^l|^2 \mid \mathbf{X}_k) = \int_0^\infty p(|z_k^l|^2 \mid \rho_k, \mathbf{X}_k) p(\rho_k) d\rho_k. \tag{18}$$

Clearly the spatial coherence of ρ_k is lost as it is integrated independently in each cell and not over the whole likelihood. On the other hand, the calculation of integral (18) can be done analytically for *Swerling* fluctuation models of type 1 and 3, leading to simple closed-forms.

2) The multitarget case: As previously discussed, in the multitarget case the parameter $\gamma^l\left(\varphi'_{k,2:N_k}, \rho_{k,1:N_k}\right)$ still depends on the phase variables $\varphi'_{k,2:N_k}$. The likelihood must thus be obtained by marginalization over modulus $\rho_{k,1:N_k}$ and phases $\varphi'_{k,2:N_k}$:

$$p(|\mathbf{z}_k|^2 \mid \mathbf{X}_k) = \int \cdots \int_{\mathbb{R}_{\geq 0}^{N_k} \times [0,2\pi)^{N_k-1}} \prod_{l=1}^{N_c} p(|z_k^l|^2 \mid \mathbf{X}_k, \rho_{k,1:N_k}, \varphi'_{k,2:N_k}) p(\rho_{k,1:N_k}) p(\varphi'_{k,2:N_k}) d\rho_{k,1:N_k} d\varphi'_{k,2:N_k}. \tag{19}$$

As in the monotarget case, this expression is to our knowledge intractable. An heuristic solution consists then again in marginalizing independently each sample from $\varphi'_{k,2:N_k}$ and $\rho_{k,1:N_k}$ as in (18), providing

$$p(|z_k^l|^2 \mid \mathbf{X}_k) = \int \cdots \int_{\mathbb{R}_{\geq 0}^{N_k} \times [0,2\pi)^{N_k-1}} p(|z_k^l|^2 \mid \mathbf{X}_k, \rho_{k,1:N_k}, \varphi'_{k,2:N_k}) p(\rho_{k,1:N_k}) p(\varphi'_{k,2:N_k}) d\rho_{k,1:N_k} \varphi'_{k,2:N_k}. \tag{20}$$

Note, however, that contrary to the monotarget case there is in general no closed-form for the integral (20), so that numerical integration must still be performed.

Finally, as with complex measurements, target contributions can often be separated so that the multitarget likelihood then resorts to a product of monotarget likelihoods. This separation is obtained under the condition $h_{k,i}^l h_{k,j}^l \approx 0, \forall i,j, i \neq j$ that permits to eliminate all cross terms in Eq.(14). It can be obtained for instance when targets are far apart enough so that their respective contributions do not overlap spatially.

IV. Likelihood computation for Swerling models

In this section, we will derive the measurement likelihood with three different *Swerling* models: *Swerling* 0, *Swerling* 1 and *Swerling* 3. For each model, we will consider first the case of complex measurements and second the case of squared modulus measurements. Whenever closed-forms are not obtainable, we will propose approximations that permit to compute the likelihood at a lower cost.

A. Complex measurements

1) Swerling 0 case: The modulus $\rho_{k,i}$ of each target is assumed constant and equal to ρ_i. Although these constants are unknown, they can be estimated over time and their estimates injected into the likelihood. For instance, in particle filter, amplitude parameters $\rho_{1:N_k}$ can be inserted in the state vector, with artificial Markovian dynamics, and sampled as the other state parameters [21]. Then integral (4) that corresponds to the complex measurement likelihood must just be computed over parameters $\varphi_{k,1:N_k}$. In the general multi-target case, this integral is, according to our knowledge, intractable and must be approximated except for the particular single target case. A first solution consists in calculating numerically the integral over the domain $[0,2\pi)^{N_k}$ but this may become rapidly computationally demanding. Thus, we propose to replace the intractable likelihood by its Laplace approximation

that has been already successfully used in particle filter application [22]. Let $\mathbf{H}_k = [\rho_1 \mathbf{h}_{k,1}, \ldots, \rho_{N_k} \mathbf{h}_{k,N_k}]$ and let $\Psi_k = [e^{j\varphi_{k,1}}, \ldots, e^{j\varphi_{k,N_k}}]^T$. Equation (4) can be rewritten as follows:

$$p\left(\mathbf{z}_k \mid \mathbf{X}_k\right) \propto \int_{[0,2\pi)^{N_k}} \exp\left\{\Upsilon\left(\varphi_{k,1:N_k}\right)\right\} d\varphi_{k,1:N_k}. \tag{21}$$

where

$$\Upsilon\left(\varphi_{k,1:N_k}\right) = -\sum_{i=1}^{N_k} \rho_i^2 \mathbf{h}_{k,i}^H \mathbf{\Gamma}^{-1} \mathbf{h}_{k,i} + \sum_{i=1}^{N_k} 2\rho_i |\mathbf{h}_{k,i}^H \mathbf{\Gamma}^{-1} \mathbf{z}_k| \cos\left(\varphi_{k,i} - \xi_{k,i}\right) - \sum_{i=1}^{N_k} \sum_{l=i+1}^{N_k} 2\rho_i \rho_l \left|\mathbf{h}_{k,i}^H \mathbf{\Gamma}^{-1} \mathbf{h}_{k,l}\right| \cos\left(\varphi_{k,i} - \varphi_{k,l} - \phi_{k,il}\right).$$

The integral (21) can be approximated using the Laplace's method [22] and is then given by

$$p_{SW0}\left(\mathbf{z}_k \mid \mathbf{X}_k\right) \approx \exp\left\{\Upsilon\left(\widehat{\varphi}_{k,1:N_k}\right)\right\} \frac{(2\pi)^{\frac{N_r}{2}}}{\left|\det\left(-\nabla^2 \Upsilon\left(\widehat{\varphi}_{k,1:N_k}\right)\right)\right|^{\frac{1}{2}}}, \tag{22}$$

where $\widehat{\varphi}_{k,1:N_k}$ is the maximum of function $\Upsilon\left(.\right)$ and $\nabla^2 \Upsilon\left(\widehat{\varphi}_{k,1:N_k}\right)$ is the Jacobian matrix calculated at the maximum. This maximum cannot be obtained analytically even for two targets and an optimization method such as a gradient descent must be used. However, this optimization step can be avoided by using the classic least square estimator

$$\widehat{\Psi}_k = \left(\mathbf{H}_k^H \mathbf{\Gamma}^{-1} \mathbf{H}_k\right)^{-1} \mathbf{H}_k^H \mathbf{\Gamma}^{-1} \mathbf{z}_k \tag{23}$$

of the complex amplitude and approximating each component by

$$\widehat{\varphi}_{k,i} = \arg\left(\widehat{\Psi}_{k,i}\right). \tag{24}$$

In practice, this estimator is in most of the situations close to the actual maximum. However, in some situations, for instance when components $\mathbf{h}_{k,1:N_k}$ are almost colinear, the difference can be greater. In that latter case, an optimization must be performed or the filter will loss in sensitivity. A compromise must then be done between the quality of the estimate and the computational time required to reach it.

2) Swerling 1 case: Each modulus $\rho_{k,i}$ follows a Rayleigh distribution:

$$p_{SW1}\left(\rho_{k,i}\right) = \frac{\rho_k}{\sigma_{\rho_i}^2} \exp\left(-\frac{\rho_{k,i}^2}{2\sigma_{\rho_i}^2}\right) \tag{25}$$

where σ_{ρ_i} is the parameter of the Rayleigh distribution such that $\mathbb{E}[\rho_{k,i}^2] = 2\sigma_{\rho_i}^2$, while the phases $\varphi_{k,1:N_k}$ are uniformly distributed over $[0, 2\pi)$. As for the *Swerling* 0 case, this parameter is unknown but it can be added to state vector as proposed in [21]. Although the integral (4) with respect to the *Swerling* 1 densities for parameters $\rho_{k,1:N_k}$ seems to be intractable directly, in practice the density $p(\mathbf{z}_k \mid \mathbf{X}_k)$ can be obtained using other probabilistic considerations. Indeed, in the *Swerling* 1 model, since $\rho_{k,i}$ follows a Rayleigh distribution of parameter $\sigma_{\rho,i}$ and $\varphi_{k,i}$ is uniformly distributed over $[0, 2\pi)$, each variable $\rho_{k,i} e^{j\varphi_{k,i}}$ in the measurement equation (1) is a zero-mean circular symmetric complex Gaussian variable with variance $2\sigma_{\rho,i}^2$. Therefore $\mathbf{z}_k$, which is then the sum of independent

Gaussian vectors with zero-mean, is a complex Gaussian vector with zero-mean and covariance matrix $\mathbf{\Sigma}_{N_k}$ given by

$$\mathbf{\Sigma}_{N_k} = \mathbf{\Gamma} + \sum_{i=1}^{N_k} 2\sigma_{\rho,i}^2 \mathbf{h}_{k,i}\mathbf{h}_{k,i}^H. \tag{26}$$

Clearly, this matrix is definite positive, so that the multi-target likelihood is finally given in closed form by:

$$p_{SW1}\left(\mathbf{z}_k \mid \mathbf{X}_k\right) \propto \frac{1}{\det\left(\mathbf{\Sigma}_{N_k}\right)} \exp\left(-\mathbf{z}_k^H \mathbf{\Sigma}_{N_k}^{-1} \mathbf{z}_k\right). \tag{27}$$

In practice, the computation of the likelihood requires the evaluation of $\det\left(\mathbf{\Sigma}_{N_k}\right)$ and $\mathbf{\Sigma}_{N_k}^{-1}$ that can be computationally demanding since matrix $\mathbf{\Sigma}_{N_k}$ is a square matrix of size equal to the length of considered vector $\mathbf{h}_{k,i}$. Fortunately, these quantities can be easily computed by using classic linear algebra formulas. Indeed, the matrix $\mathbf{\Sigma}_{N_k}$ can be written

$$\mathbf{\Sigma}_{N_k} = \mathbf{\Gamma} + \mathbf{U}\mathbf{V}\mathbf{U}^H, \tag{28}$$

where $\mathbf{U} = [\mathbf{h}_{k,1}, \cdots, \mathbf{h}_{k,N_k}]$ is a matrix with N_k columns and $\mathbf{V} = diag\left(2\sigma_{\rho,1}^2, \cdots, 2\sigma_{\rho,N_k}^2\right)$. Then using a classic matrix inversion lemma (see [23], p. 117), it comes

$$\mathbf{\Sigma}_{N_k}^{-1} = \mathbf{\Gamma}^{-1} - \mathbf{\Gamma}^{-1}\mathbf{U}\left(\mathbf{V}^{-1} + \mathbf{U}^H\mathbf{\Gamma}^{-1}\mathbf{U}\right)^{-1}\mathbf{U}^H\mathbf{\Gamma}^{-1}. \tag{29}$$

The inverse of matrix $\mathbf{\Gamma}$ can be pre-computed, while $\mathbf{V}$ is a diagonal matrix and matrix $\left(\mathbf{V}^{-1} + \mathbf{U}^H\mathbf{\Gamma}^{-1}\mathbf{U}\right)$ is an N_k-by-N_k matrix of much smaller size than $\mathbf{\Sigma}_{N_k}$ as long as the number of targets N_k remains small compared to the number of considered cells. In that case its inversion implies a drastically reduced cost compared to the inversion of $\mathbf{\Sigma}_{N_k}$. Furthermore, the computational cost of the determinant can also be reduced using the matrix determinant lemma (see [23], p. 117)

$$\det\left(\mathbf{\Sigma}_{N_k}\right) = \det\left(\mathbf{V}^{-1} + \mathbf{U}^H\mathbf{\Gamma}^{-1}\mathbf{U}\right)\det\left(\mathbf{V}\right)\det\left(\mathbf{\Gamma}\right). \tag{30}$$

Note that no hypothesis was made here about the closeness of the targets and therefore this closed-form expression is valid both for distant and close targets. Finally, for the particular monotarget case, the likelihood simply becomes

$$p_{SW1}\left(\mathbf{z}_k \mid \mathbf{X}_k\right) \propto \frac{1}{1 + 2\sigma_\rho^2 \mathbf{h}_k^H\mathbf{\Gamma}^{-1}\mathbf{h}_k} \exp\left(\frac{2\sigma_\rho^2 |\mathbf{h}_k^H\mathbf{\Gamma}^{-1}\mathbf{z}_k|^2}{1 + 2\sigma_\rho^2 \mathbf{h}_k^H\mathbf{\Gamma}^{-1}\mathbf{h}_k}\right). \tag{31}$$

3) Swerling 3 case: Each squared modulus $\rho_{k,i}^2$ follows a chi-square distribution with four degrees of freedom so that the corresponding density for the modulus $\rho_{k,i}$ is provided by:

$$p_{SW3}\left(\rho_{k,i}\right) = \frac{8\rho_{k,i}^3}{\nu_{\rho_i}^2} \exp\left(-\frac{2\rho_{k,i}^2}{\nu_{\rho_i}}\right), \tag{32}$$

where the parameter ν_{ρ_i} is such that $\mathbb{E}[\rho_{k,i}^2] = \nu_{\rho_i}$. As for the *Swerling* 0 and *Swerling* 1 case, the parameter ν_{ρ_i} is unknown but can be added to the state vector [21]. According to our knowledge, no closed form can be obtained for Eq (4) in the *Swerling* 3 case and a numerical approximation must be done, implying the numerical computation of N_k integrals over modulus $\rho_{k,1:N_k}$ and N_k integrals over phases $\varphi_{k,1:N_k}$. However, it is possible to

avoid the numerical integration over the parameters $\rho_{k,1:N_k}$ by approximating the chi-square distribution by a Rice distribution; note indeed that the *Swerling* 3 model can be viewed as an approximation of a Rice distribution [24]. Using a Rice distribution instead of the *Swerling* 3 model, the density of the modulus $\rho_{k,i}$ becomes

$$p_{\text{Rice}}\left(\rho_{k,i}\right) = \frac{2\rho_{k,i}(1+a^2)}{\nu_{\rho_i}} \exp\left(-a^2 - \rho_{k,i}^2 \frac{(1+a^2)}{\nu_{\rho_i}}\right) \mathrm{I}_0\left(2a\sqrt{\rho_{k,i}^2 \frac{(1+a^2)}{\nu_{\rho_i}}}\right), \tag{33}$$

where a is the ratio between the dominant scatterer and the weaker ones. By choosing $a = \sqrt{1+\sqrt{2}}$, it can be easily checked that densities of the squared modulus $\rho_{k,i}^2$ under *Swerling* 3 and Rice models provide the same means and variances [24]. Now consider the complex amplitude $\rho_{k,i}e^{j\varphi_{k,i}}$ where $\rho_{k,i}$ is distributed according to the Rice distribution (33). Recall first that this Rice distribution is the distribution of the modulus of a complex Gaussian variable with mean $\mu_{SW3,i} = a\sqrt{\frac{\nu_{\rho_i}}{(1+a^2)}}$ and variance $2\sigma_{SW3,i}^2 = \frac{\nu_{\rho_i}}{(1+a^2)}$.

Then we can replace each variable $\rho_{k,i}e^{j\varphi_{k,i}}$ in (1) by a variable $\xi_{k,i}e^{j\psi_{k,i}}$ where the variables $\xi_{k,i}$ and $\psi_{k,i}$ are respectively Gaussian and uniform, and such that $\xi_{k,i}e^{j\psi_{k,i}}$ follows the same distribution as $\rho_{k,i}e^{j\varphi_{k,i}}$. Then, conditionally to phases $\psi_{k,1:N_k}$, the observation $\mathbf{z}_k$ is a complex Gaussian vector with mean

$$\boldsymbol{\mu}_{k,SW3} = \sum_{i=1}^{N_k} \mu_{SW3,i} e^{j\psi_{k,i}} \mathbf{h}_{k,i}$$

and covariance matrix

$$\boldsymbol{\Phi}_{N_k} = \boldsymbol{\Gamma} + \sum_{i=1}^{N_k} 2\sigma_{SW3,i}^2 \mathbf{h}_{k,i}\mathbf{h}_{k,i}^H.$$

The density is then given by,

$$p_{\text{Rice}}\left(\mathbf{z}_k \mid \mathbf{X}_k, \psi_{k,1:N_k}\right) \propto \frac{1}{\det\left(\boldsymbol{\Phi}_{N_k}\right)} \exp\left(-\left(\mathbf{z}_k - \boldsymbol{\mu}_{k,SW3}\right)^H \boldsymbol{\Phi}_{N_k}^{-1} \left(\mathbf{z}_k - \boldsymbol{\mu}_{k,SW3}\right)\right) \tag{34}$$

Clearly, the computational cost of $\boldsymbol{\Phi}_{N_k}^{-1}$ and $\det\left(\boldsymbol{\Phi}_{N_k}\right)$ can be reduced as in the *Swerling* 1 case. Then, it just remains to marginalize (34) over the phases $\psi_{k,1:N_k}$. This marginalization cannot be computed analytically and must then be calculated numerically, except in the monotarget case.

In the particular monotarget case, a closed-form can be obtained both for the chi-square distribution and the Rice distribution. For the chi-square distribution, the expression in Eq.(10) must be integrated over density (32). The following result (see [25], p. 1097 Eq. 6.663)

$$\int_0^{+\infty} x^3 \exp\left(-\alpha x^2\right) \mathrm{I}_0\left(\beta x\right) dx = \frac{2}{\alpha^2}\left(1 + \frac{\beta}{4\alpha}\right) \exp\left(\frac{\beta^2}{4\alpha}\right), \tag{35}$$

where $\alpha \in \mathbb{R}_{\geq 0}^*$ and $\beta \in \mathbb{R}$, is used with $\alpha = \frac{2}{\nu_\rho} + \mathbf{h}_k^H \boldsymbol{\Gamma}^{-1} \mathbf{h}_k$ and $\beta = 2\left|\mathbf{h}_k^H \boldsymbol{\Gamma}^{-1} \mathbf{z}_k\right|$. Then, the likelihood for the chi-square *Swerling* 3 model in the monotarget case is given by

$$p_{SW3}\left(\mathbf{z}_k \mid \mathbf{X}_k\right) \propto \frac{4}{\left(2 + \nu_\rho \mathbf{h}_k^H \boldsymbol{\Gamma}^{-1} \mathbf{h}_k\right)^2} \left(1 + \frac{\nu_\rho \left|\mathbf{h}_k^H \boldsymbol{\Gamma}^{-1} \mathbf{z}_k\right|}{2 + \nu_\rho \mathbf{h}_k^H \boldsymbol{\Gamma}^{-1} \mathbf{h}_k}\right) \exp\left(\frac{\nu_\rho \left|\mathbf{h}_k^H \boldsymbol{\Gamma}^{-1} \mathbf{z}_k\right|^2}{2 + \nu_\rho \mathbf{h}_k^H \boldsymbol{\Gamma}^{-1} \mathbf{h}_k}\right). \tag{36}$$

For the Rice distribution, it is possible to integrate Eq.(34) over the phase ψ, a computation similar to the one providing Eq.(10), Then, the likelihood for the Rice *Swerling* 3 model in the monotarget setting is given by

$$p_{\text{Rice}}\left(\mathbf{z}_k \mid \mathbf{X}_k\right) \propto \frac{\left(1+a^2\right)\exp\left(-a^2\right)}{1 + a^2 + \nu_\rho \mathbf{h}_k^H \boldsymbol{\Gamma}^{-1} \mathbf{h}_k} \exp\left(\frac{\nu_\rho \left|\mathbf{h}_k^H \boldsymbol{\Gamma}^{-1} \mathbf{z}_k\right|^2 + a^2\left(1+a^2\right)}{1 + a^2 + \nu_\rho \mathbf{h}_k^H \boldsymbol{\Gamma}^{-1} \mathbf{h}_k}\right) \mathrm{I}_0\left(\frac{2a\left|\mathbf{h}_k^H \boldsymbol{\Gamma}^{-1} \mathbf{z}_k\right| \sqrt{\left(1+a^2\right)\nu_\rho}}{1 + a^2 + \nu_\rho \mathbf{h}_k^H \boldsymbol{\Gamma}^{-1} \mathbf{h}_k}\right). \tag{37}$$

B. Squared modulus measurements

As we have seen, the likelihood computation with the squared modulus can be done in two ways, either by taking into account the spatial coherence of the phases and modulus with Eq.(19) or by marginalizing independently in each cell with Eq.(20). As this two cases are different we treat them separately in the following.

1) The coherent case: In the coherent case, the likelihood is obtained according to Eq.(19) by replacing the generic density $p\left(\rho_{k,i}\right)$ by the density of the fluctuation considered. However, according to our knowledge, it cannot be done analytically for the *Swerling* models and the integral must be approximated numerically. Moreover, Note that it can be really intensive in terms of computational resources especially when the number of target is large since the size of the integration domain increases exponentially with the number of targets. For this reason, we propose an heuristic solution that consists in replacing the parameter $\gamma^l\left(\rho_{k,1:N_k},\varphi_{k,2:N_k}\right)$ by its expectation

$$\mathbb{E}[\gamma^l\left(\rho_{k,1:N_k},\varphi_{k,2:N_k}\right)] = \sum_{i=1}^{N_k} \frac{\mathbb{E}\left[\rho_i^2\right]\left|h_{k,i}^l\right|^2}{\sigma^2}, \tag{38}$$

where $\mathbb{E}\left[\rho_i^2\right]$ just depends on the parameter of the fluctuations density. Thus, integrals (19) are just the product of the densities in Eq.(11) for all the cells. This is a strong approximation for the likelihood, but as you will see in V, it gives interesting performance and it is really faster than the numerical integration which is costly in terms of computational resources. In the monotarget case, the likelihood is given by Eq.(16) that requires the integration only over parameter ρ_k and therefore the numerical approximation can be done in a reasonable time.

2) The non coherent case: The non coherent case consists in calculating Eq.(20). In practice for the *Swerling* 0 case, it has no interest and Eq.(19) must be used as it takes into account the spatial coherence of variables $\varphi_{k,2:N_k}$. Nevertheless, for the *Swerling* 1 and 3 cases, probabilistic considerations can be used to calculate Eq.(20). Indeed, in the *Swerling* 1 case Boers *et al.* [10] noticed that sample $|z_k^l|^2$ follows an exponential distribution with parameter $\lambda_k^l = \frac{1}{2\sigma^2+\sum_{i=1}^{N_k} 2\sigma_{\rho_i}^2 |h_k^l|^2}$, so that

$$p(|z_k^l|^2 \mid \mathbf{X}_k) = \frac{1}{\lambda_k^l} \exp\left(-\frac{|z_k^l|^2}{\lambda_k^l}\right). \tag{39}$$

For the *Swerling* 3 case, the integration over parameters $\rho_{k,1:N_k}$ can be avoided with the Rice fluctuations. Indeed, by replacing each variable $\rho_{k,i}e^{j\varphi_{k,i}}$ by a variable $\xi_{k,i}e^{j\psi_{k,i}}$, each sample

$$\frac{|z_k^l|^2}{\sigma^2 + \sum_{i=1}^{N_k} \sigma_{SW3,i}^2 \left|h_k^l\right|^2}$$

conditionally on variables $\psi_{k,1:N_k}$ follows a non central chi-square distribution with two degrees of freedom; with non-centrality parameter

$$\gamma_{\text{Rice}}^l\left(\psi'_{k,2:N_k}\right) = \frac{\left|\mu_{SW3,1}h_{k,1}^l + \sum_{i=2}^{N_k} \mu_{SW3,i}e^{j\psi'_{k,i}}h_{k,i}^l\right|^2}{\sigma^2 + \sum_{i=1}^{N_k} \sigma_{SW3,i}^2 \left|h_k^l\right|^2}, \tag{40}$$

that does not depend on parameters $\rho_{k,1:N_k}$ anymore. The density of $|z_k^l|^2$ conditionally on $\psi'_{k,2:N_k}$ is given by Eq. (13) where σ^2 is substituted by $\sigma^2 + \sum_{i=1}^{N_k} \sigma_{SW3,i}^2 \left|h_k^l\right|^2$ and $\gamma^l\left(\varphi'_{k,2:N_k}, \rho_{k,1:N_k}\right)$ by $\gamma^l_{\text{Rice}}\left(\psi'_{k,2:N_k}\right)$. Finally the likelihood $|z_k^l|^2$ is obtained only by integrating over variables $\psi'_{k,2:N_k}$.

In the monotarget case integral (18) can be computed analytically both for the Rice distribution and the chi-square. For the Rice distribution, no integration over phase $\psi'_{k,1}$ is required and the likelihood is given by

$$p_{SW3,\text{Rice}}\left(\left|z_k^l\right|^2 \mid \mathbf{X}_k\right) \propto \frac{2\sigma^2(1+a^2)\exp\left(-a^2\right)}{2\sigma^2(1+a^2)+\nu_\rho\left|h_k^l\right|^2} \exp\left(\frac{\nu_\rho \frac{\left|h_k^l\right|^2\left|z_k^l\right|^2}{2\sigma^2} + 2\sigma^2 a^2\left(1+a^2\right)}{2\sigma^2\left(1+a^2\right)+\nu_\rho\left|h_k^l\right|^2}\right) \mathrm{I}_0\left(\frac{2a\left|h_k^l\right|\left|z_k^l\right|\sqrt{(1+a^2)\,\nu_\rho}}{1+a^2+\nu_\rho\left|h_k^l\right|^2}\right). \tag{41}$$

For the chi-square distribution, result (35) is used with $\alpha = \frac{\nu_\rho\left|h_k^l\right|^2+4\sigma^2}{2\nu_\rho\sigma^2}$ and $\beta = \frac{\left|h_k^l\right|\left|z_k^l\right|}{\sigma^2}$. Then, integral (18) becomes

$$p_{SW3,\chi^2}\left(\left|z_k^l\right|^2 \mid \mathbf{X}_k\right) \propto \frac{\left(4\sigma^2\right)^2}{\left(4\sigma^2+\nu_\rho\left|h_k^l\right|^2\right)^2}\left(1+\frac{\left|z_k^l\right|^2}{2\sigma^2}\frac{\nu_\rho\left|h_k^l\right|^2}{4\sigma^2+\nu_\rho\left|h_k^l\right|^2}\right)\exp\left(\frac{\left|z_k^l\right|^2}{2\sigma^2}\frac{\nu_\rho\left|h_k^l\right|^2}{4\sigma^2+\nu_\rho\left|h_k^l\right|^2}\right) \tag{42}$$

C. Summary

In this section, we have given several way to compute the likelihood in a Track-Before-Detect context for complex amplitudes fluctuation of type *Swerling* 0, 1 and 3. For the computation of the Likelihood with the complex measurement, we have shown that a closed-form can be obtained for all the *Swerling* fluctuations considered in the monotarget case. In the multitarget case, a closed-form can be obtained only in the *Swerling* 1 case, in the other cases a numerical integration must be performed, however we propose several methods in order to alleviate the time calculation. For the Likelihood with the squared modulus of the complex measurement, we have derived the right expression in order to keep the spatial coherence information of complex amplitude parameters and we have shown that only the dependency of one phase can be removed, however this leads to an intractable integral for all the *Swerling* models. Then approximation must be performed and we give the principal way to do so. In table IV, we give a sum-up of the different techniques to calculate the likelihood with the existing methods on those proposed in this article.

V. Simulation and Results

In this section, we first study the performance in detection and estimation of a single target particle filter that considers either complex measurements or squared modulus. We show the improvement of using complex measurements both in detection and in estimation only for the *Swerling* 1 and 3 model as Davey *et al.* have already shown the benefits of doing so in the *Swerling* 0 case. Then, we study the behaviour of a simple multitarget particle filter for two close targets. Performance are evaluated in terms of estimation of the two target states and track loss for fluctuations of type *Swerling* 0, 1 and 3.

A. Target Model

We assume a discrete time model, with a fixed time step T, and we define the state vector of the i^{th} target as $\mathbf{x}_{k,i} = [x_{k,i}, \dot{x}_{k,i}, y_{k,i}, \dot{y}_{k,i}]^T$, where $(x_{k,i}, y_{k,i})$ and $(\dot{x}_{k,i}, \dot{y}_{k,i})$ are, respectively, the location and the velocity of

the target in Cartesian coordinates. If the i^{th} target appears at step k, its position $(x_{k,i}, y_{k,i})$ is uniformly drawn in the pavement defined in polar coordinate $\mathcal{P} = [r_{min}, r_{max}] \times [\theta_{min}, \theta_{max}]$ where r_{min}, r_{max}, θ_{min} and θ_{max} are respectively the minimum and maximum target ranges and bearings. The velocity $(\dot{x}_{k,i}, \dot{y}_{k,i})$ is uniformly drawn in the area $\mathcal{C} = \{(\dot{x}_k, \dot{y}_k) \mid v_{min} \leqslant \sqrt{\dot{x}_k^2 + \dot{y}_k^2} \leqslant v_{max}\}$ where v_{min} and v_{max} are respectively the minimum and maximum target velocity. On the contrary, if the i^{th} target was already present at previous step $k-1$, we assume that the target state evolves according to the following linear equation:

$$\mathbf{x}_{k,i} = \mathbf{F}\mathbf{x}_{k-1,i} + \mathbf{v}_{k,i}, \tag{43}$$

where $\mathbf{v}_{k,i}$ is a white Gaussian noise with covariance matrix

$$\mathbf{Q} = \begin{bmatrix} \mathbf{Q}_s & 0 \\ 0 & \mathbf{Q}_s \end{bmatrix}, \text{ with } \mathbf{Q}_s = q_s \begin{bmatrix} \mathrm{T}^3/3 & \mathrm{T}^2/2 \\ \mathrm{T}^2/2 & \mathrm{T} \end{bmatrix},$$

and $\mathbf{F}$ is the transition matrix defined by:

$$\mathbf{F} = \begin{bmatrix} \mathbf{F}_s & 0 \\ 0 & \mathbf{F}_s \end{bmatrix} \text{ with } \mathbf{F}_s = \begin{bmatrix} 1 & \mathrm{T} \\ 0 & 1 \end{bmatrix}.$$

Concerning the modulus, we consider fluctuations of type *Swerling* 0, 1 and 3 with parameters ρ_i, $2\sigma_{\rho_i}^2$ and ν_{ρ_i} respectively.

B. Ambiguity function

In Eq.(1), the ambiguity function $\mathbf{h}_k(\mathbf{x}_k)$ is possibly multidimensional depending on the radar application under consideration. We consider here a simple scenario with only range and bearing measurements.For the range, the transmitted pulse is assumed to be a linear frequency modulated signal ("chirp") with band B and duration T_e, whose range ambiguity function is given by [26]:

$$h_r^l(\mathbf{x}_k) = \frac{\sin\left(\pi B\tau^l\left(1 - \frac{|\tau^l|}{T_e}\right)\right)}{\pi B\tau^l} \text{ for } |\tau^l| \leq T_e,$$

with $\tau^l = 2\left(r_k - r_l\right)/c$, c the celerity of the electromagnetic wave, $r_k = \sqrt{x_k^2 + y_k^2}$ and $r_l = r_{min} + (l + \frac{1}{2})\Delta_r$, $l \in [0, N_r - 1]$ with $\Delta_r = \frac{c}{2B}$ the range resolution and $N_r = \left\lceil \frac{r_{max} - r_{min}}{\Delta_r} \right\rceil$. For the bearing, we consider at the reception a linear phased array of N_a antennas spaced by $\frac{\lambda}{2}$ (where λ is the wavelength of the carrier frequency). Then the ambiguity in bearing is given by [27],

$$h_\theta^m(\mathbf{x}_k) = \frac{\sin\left(\frac{N_a\Phi^m}{2}\right)}{N_a \sin\left(\frac{\Phi^m}{2}\right)},$$

with $\Phi^m = \frac{2\pi d_a}{\lambda}\left[\cos(\theta_k) - \cos\left(\theta_m\right)\right]$, $\theta_k = \arctan(\frac{y_k}{x_k})$ the target bearing and $\theta_m = \theta_{min} + (m + \frac{1}{2})\Delta_\theta$, $m \in [0, N_\theta - 1]$ with $\Delta_\theta = 1.772\frac{\lambda}{N_a}$ the half-power beamwidth [27] and $N_\theta = \left\lceil \frac{\theta_{max} - \theta_{min}}{\Delta_\theta} \right\rceil$.

The overall range-bearing ambiguity function in cell (l, m) is given by the product $h^{lm}(\mathbf{x}_k) = h_r^l(\mathbf{x}_k) \times h_\theta^m(\mathbf{x}_k)$. Finally $\mathbf{h}_k(\mathbf{x}_k)$ is a vector of size $N_c = N_r \times N_\theta$ defined by

$$\mathbf{h}_k(\mathbf{x}_k) = \left[h^{11}(\mathbf{x}_k), h^{12}(\mathbf{x}_k), \cdots, h^{12}(\mathbf{x}_k), \cdots, h^{N_r N_\theta}(\mathbf{x}_k)\right].$$

The noise covariance matrix is assumed to be $\mathbf{\Gamma} = 2\sigma^2\mathbf{I}_{N_c}$. Throughout this section, the SNR will be defined by $\text{SNR} = 10\log_{10}\left(\frac{\mathbb{E}[\rho_k^2]}{2\sigma^2}\right)$. Note that this definition provides a simple relationship between the fluctuation parameters ρ, σ_ρ and ν_ρ and the target SNR and in the following we will always give the SNR instead of the value of the parameter. Note also that in practice, the ambiguity function have only significant values in a small set of cells around the target location. Therefore, to avoid unnecessary computation, it can be advantageous to truncate the function $\mathbf{h}(\mathbf{x}_k)$ and compute the likelihood only in the set of cells $\mathcal{V}_{\mathbf{x}_k}$ where the ambiguity function remains significant [8]. For a target located in cell (l, m), we define $\mathcal{V}_{\mathbf{x}_k}$ as,

$$\mathcal{V}_{\mathbf{x}_k} = \{(u, v) \mid |l - u| \leq \delta_r, \text{ and } |m - v| \leq \delta_\theta\}, \tag{44}$$

In the rest of the paper, $\mathbf{h}(\mathbf{x}_k)$ will thus be computed only over the set of cells $\mathcal{V}_{\mathbf{x}_k}$. Furthermore, note that in that case and with $\mathbf{\Gamma} = 2\sigma^2\mathbf{I}_{N_c}$, condition (5) holds when

$$\mathcal{V}_{\mathbf{x}_{k,u}} \cap \mathcal{V}_{\mathbf{x}_{k,v}} = \varnothing, \ \forall(u, v), \ u \neq v.$$

C. Single Target Simulation and Results

1) Scenario of the Simulation: We consider a scenario with 100 time steps. The target appears at time step $k_b = 10$ and disappears at step $k_d = 75$. At time step k_b, the target state is initialized with the prior distribution defined in section V-A and until time step k_d the state is propagated according to (43) (with $q_s = 0$). We also assume that the entire trajectory is contained within area $\mathcal{P}$. The SNR of the target is fixed to 5dB and we consider fluctuations of type *Swerling* 1 and 3.

2) Single Target Particle Filter: For the simulations, we consider the TBD monotarget particle filter described in [14]. In the following, we briefly recall the principle of this filter. To perform the detection stage, a Markovian variable s_k is added to the state vector and takes the value 1 if the target is present and 0 otherwise. Thus, the process $(s_k)_{k\in\mathbb{N}}$ is entirely defined by its transition probabilities $P_b = p(s_k = 1 \mid s_{k-1} = 0)$ (birth probability) and $P_d = p(s_k = 0 \mid s_{k-1} = 1)$ (death probability). The probability of presence $p(s_k = 1 \mid \mathbf{z}_{1:k})$ can be computed recursively and allows to make a decision about the target presence in the radar window. Moreover, as we have already mentioned, parameter $2\sigma_\rho^2$ for the *Swerling* 1 case is unknown and so it is added to the particle state as proposed in [21]. Obviously this parameter is replaced by $\nu_{k,p}$ in the *Swerling* 3 case. At step $k-1$, the particle filter consists of a set of N_{co} particles (continuing particles) with uniform weights $\left\{\frac{1}{N_{co}}, \mathbf{x}_{k-1}^p\right\}_{p=1,\cdots,N_{co}}$ that are propagated according to Eq.(43). For the modulus parameter, it is simply propagated according to

$$2\sigma_{k,p}^2 = 2\sigma_{k-1,p}^2 + n_k, \tag{45}$$

where v_k is Gaussian noise, with variance σ_n.

Then N_b new particles (birth particles) are initialized in the radar window. Note that using the uniform prior density for the particle initialization leads to poor performance. Therefore we resort here to the method proposed in [28] that initializes the particle location (x_k^p, y_k^p) in cells exceeding a given threshold $\nu_{P_{fa}} = -2\sigma^2\log(P_{fa})$

(where P_{fa} is a given false alarm probability). Concerning the velocity, we simply choose a uniform prior over the area $\mathcal{C}$ defined in V-A. Finally, parameters $\sigma^2_{0,p}$ and $\nu_{0,p}$ are drawn uniformly over the interval corresponding to a target SNR between SNR_{min} and SNR_{max}.

The approximated posterior density is a mixture with two components, one for the birth particles and one for the continuing particles. Therefore unnormalized weights are calculated separately. For the birth particles it is given by

$$\tilde{w}^p_{k,b} \propto \frac{N_{P_{fa}}}{N} \times \frac{1}{N_b} p\left(\mathbf{z}_k \mid \mathbf{x}^p_k\right), \tag{46}$$

where $N_{P_{fa}}$ is the number of cells exceeding the threshold $\nu_{P_{fa}}$. For the continuing particles it is given by

$$\tilde{w}^p_{k,c} \propto \frac{1}{N_c} p\left(\mathbf{z}_k \mid \mathbf{x}^p_k\right). \tag{47}$$

Finally, The probability of each component is given by

$$\begin{aligned} p_c &= \frac{\tilde{M}_c}{\tilde{M}_c + \tilde{M}_b}, \\ p_b &= 1 - p_c, \end{aligned} \tag{48}$$

where

$$\begin{aligned} \tilde{M}_c &= (1 - P_d)\hat{P}^e_{k-1} \sum_{p=1}^{N_{co}} \tilde{w}^c_{k,p}, \\ \tilde{M}_b &= P_b(1 - \hat{P}^e_{k-1}) \sum_{q=1}^{N_b} \tilde{w}^b_{k,q}, \end{aligned} \tag{49}$$

with $\hat{P}^e_{k-1}$ the estimated probability of target existence at step $k-1$. The estimated probability $\hat{P}^e_k$ of target existence is obtained by

$$\hat{P}^e_k = \frac{\tilde{M}_c + \tilde{M}_b}{\tilde{M}_c + \tilde{M}_b + P_d\hat{P}^e_{k-1} + (1 - P_b)(1 - \hat{P}^e_{k-1})}. \tag{50}$$

The weights are normalized separately for the birth and continuing particles. Finally, N_c particles are resampled from the $N_{co} + N_b$ particle cloud.

3) Detection scheme: The proposed particle filter allows to estimate the probability of existence $\hat{P}^e_k$ but does not take any decision on the presence or absence of the target. It appears that a common detection scheme consists in simply thresholding the probability of existence. However, this way of proceed can lead to miss detections. Indeed for an outlier measurement $\mathbf{z}_k$, the estimated probability of existence $\hat{P}^e_k$ may become pretty small in one iteration, even though particles are properly located around the target; in that case the target will not be detected at that iteration. To avoid this issue, we use an adaptive threshold that depends on the detection status of the target at previous step.

Let us thus call d_k the decision at time step k that can take value 0 (no detection) or 1 (detection), the following detection scheme is used:

$$d_k = \begin{cases} 1 & \text{if } \hat{P}^e_k > T_h(d_{k-1}), \\ 0 & \text{otherwise.} \end{cases} \tag{51}$$

At step $k = 0$, we assume that $d_{-1} = 0$.

4) Simulations: For the simulation of the target scenario, the following parameters are used: SNR $= 5$dB, T=1 s, $v_{min} = 100$ m/s, $v_{max} = 300$ m/s, SNR$_{min} = 2$ dB, SNR$_{max} = 10$ dB, $q_s = 10^{-3}$, $P_{fa} = 0.1$ and $\sigma_n^2 = 0.05$. The transition probabilities for the particle filter are set to $P_b = P_d = 0.05$. The number of continuing particles is set to $N_c = 2000$ and the number of newborn particles to $N_b = 1000$. Concerning the detection strategy, we choose $T_h(d_{k-1} = 0) = 0.9$ and $T_h(d_{k-1} = 1) = 0.2$.

For the simulation of the radar measurements, the parameters used are: $r_{min} = 100$ km,$r_{max} = 120$ km $\theta_{min} = -10°$, $\theta_{max} = +10°$, $N_r = 40$, $N_\theta = 14$, $\sigma^2 = 0.5$, $B = 150$ kHz, $T_e = 6.67 \times 10^{-5}$ s, $N_a = 70$, $\lambda = 3$ cm, $c = 3 \times 10^8$ m.s^{-1}. Note that a small radar window is chosen here to avoid using an important number of particles and thus limit the computational cost.

Three filters are used to detect and estimate the hidden target state $\mathbf{x}_k$, based on different assumptions for the likelihood computation:

1) The first filter, denoted by CSM PF (Coherent Squared Modulus Particle Filter), considers squared modulus to compute the likelihood and takes into account the spatial coherence of the amplitude parameter ρ_k: it corresponds to Eq. (16).
2) The second filter, denoted by NCSM PF (Non Coherent Squared Modulus Particle Filter), considers squared modulus but does not take into account the spatial coherence of the amplitude parameter ρ_k: it corresponds to Eq. (18).
3) The third filter, denoted by CM PF (Complex Measurement Particle Filter), considers complex measurements and spatial coherence: it corresponds to Eq.(9).

$N_{MC} = 1000$ Monte-Carlo simulation were performed for performance measurement. Finally, the RMSE in position and velocity is measured when $d_k = 1$ and the estimated target location is in the detection area of two range-bearing cells from the actual target position.

a) Detection performance: In figures 2 and 3, we present the average of variable d_k is measured at each step for the *Swerling* 1 and 3 models respectively. In both case, filters that use the complex measurement outperform those that use squared modulus. Furthermore, the difference between SMCPF and SMNCPF is quite small, therefore it seems that taking into account the spatial coherence of the phase is more important than taking into account the modulus information. Moreover, SMCPF requires numerical approximation that leads to increase the computational time for a very small gain in detection.

b) Estimation performance: In figures 4 and 5, we present the result in terms of RMSE in position and velocity for the *Swerling* 1 and 3 models respectively. As for all the detection results, particle filters that used the complex measurement outperform filters that work on squared modulus. Moreover, note that the RMSE in position seems to be better at the beginning which is not expected since the tracking alogrithm should improve the RMSE. However, this can be explained by the fact that the RMSE is calculated only over the iteration where the target has been detected (*i.e.* $d_k = 1$) and at the beginning only a few simulations have detected the target (recall the SNR of 5dB used here). These detections correspond to favorable cases After a few iteration, target has been detected in most of

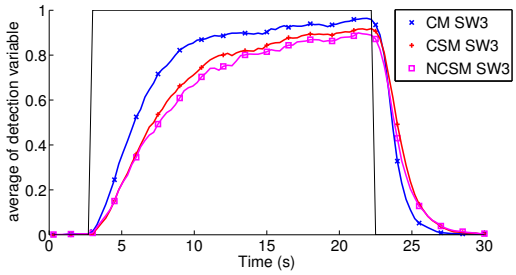

Fig. 2. Monte-Carlo simulation results for the single target case with the *Swerling* 1 model. average of the detection variable d_k. SNR $= 5$ dB.

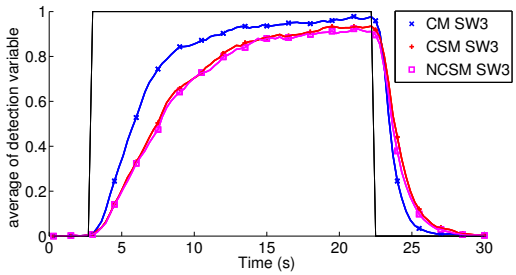

Fig. 3. Monte-Carlo simulation results for the single target case with the *Swerling* 3 model. average of the detection variable d_k. SNR $= 5$ dB.

the case and thus particularly cases where it is located at the edge of the cell and thus it has lost of few dB, which leads to increase the RMSE. Besides with the filter used here, some birth particles are spread everywhere in the observation window, and used for the situation as well, thus leading to an increase in the RMSE. This phenomena could be managed by clustering the particle cloud before the estimate computation.

D. Multi-Target Simulation and Results

1) Multi-Target Scenario: We now consider a scenario with two targets present during all the experiment. Both targets follow a uniform rectilinear trajectory. Target states $\mathbf{x}_{k,1}$ and $\mathbf{x}_{k,2}$ are uniformly initialized over $\mathcal{P} \times \mathcal{C}$ such that:

- the two velocity vectors $(\dot{x}_{k,1}, \dot{y}_{k,1})$, $(\dot{x}_{k,2}, \dot{y}_{k,2})$ form an angle of $\frac{\pi}{4}$.
- the minimum distance between targets is reached at time step $k_c = 35$ and is set to $d_{min} = 150$ m, *i.e.* the minimum distance is smaller than the range resolution.

Targets are set to 10dB and we consider fluctuations of type *Swerling* 0, 1 and 3.

2) Multi-Target Particle Filter: For the simulation, we consider here the particle filter proposed by Kreucher *et al.* [9]. We assume that the number of targets is known since the objective here is to measure the effect of the likelihood computation on the particle filter for two close targets. Therefore, the particle state is defined as $\mathbf{X}_k^p = [\mathbf{x}_{k,1}^p, \mathbf{x}_{k,2}^p]^T$, where $\mathbf{x}_{k,1}^p$ and $\mathbf{x}_{k,2}^p$ are the single state vectors of the first and second targets respectively of particle p, $p \in \{1, \ldots, N_p\}$. In the following, we detail the instrumental density used in the particle filter.

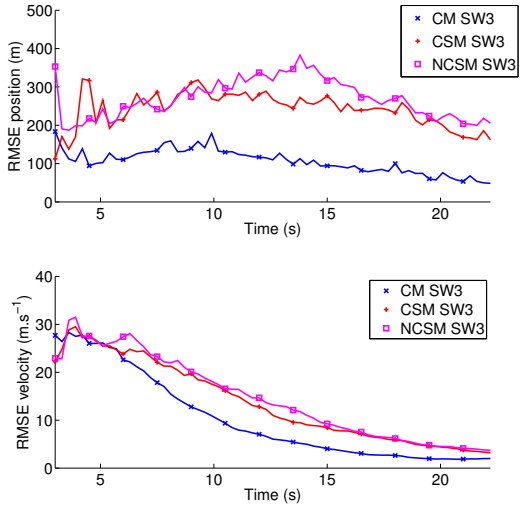

Fig. 4. Monte-Carlo simulation results for the single target case with the *Swerling* 1 model. Top: RMSE in position. Bottom: RMSE in velocity. SNR $= 5$ dB.

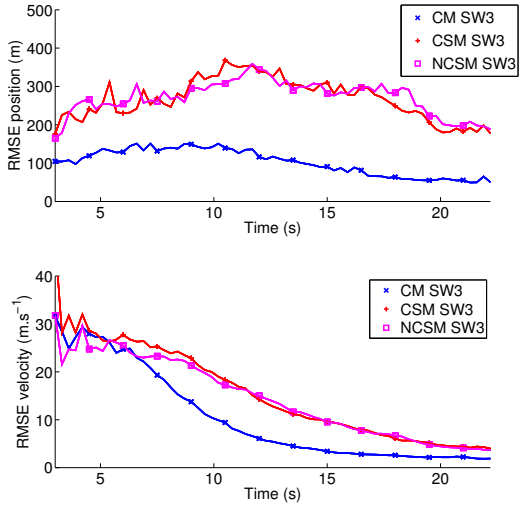

Fig. 5. Monte-Carlo simulation results for the single target case with the *Swerling* 3 model. Top: RMSE in position. Bottom: RMSE in velocity. SNR $= 5$ dB.

At step $k = 0$, each particle target state $\mathbf{x}_{0,i}^{p}$ is initialized from the actual target state according to the following procedure:

- for the position, a Gaussian noise with variance σ_r^2 is added to the actual target range $r_{0,i} = \sqrt{x_{0,i}^2 + y_{0,i}^2}$ and a Gaussian noise with variance σ_θ^2 is added to the true target bearing $\theta_{0,i} = \arctan\left(\frac{y_{0,i}}{x_{0,i}}\right)$.
- The velocity is initialized around the true velocity in Cartesian coordinates by adding a Gaussian noise with

covariance matrix $\sigma_v^2\mathbf{I}_2$.

For the particle propagation, we consider two cases:

- Either for each particle, state $\mathbf{X}_k^p$ verifies (5). Then, the likelihood for each target state $\mathbf{x}_{k,i}^p$ can be computed separately and we propose to use the Independent Partition instrumental density (IP) [9], *i.e.* sample the state of the particles according to the distributions defined by the likelihood of each target.
- Or hypothesis (5) is not verified for all the particles and (IP) cannot be used any longer. In that latter case, we just propagate particles according to the prior distribution Eq. (43).

3) Calculation of probability of track loss: The probability of track loss is evaluated from N_{MC} Monte-Carlo simulation with the following procedure: at each time step k and for each target, we compute the binary loss variable

$$l_{k,i} = \begin{cases} 1 & \text{if } \begin{pmatrix} \hat{r}_{k,i} - r_{k,i} \\ \hat{\theta}_{k,i} - \theta_{k,i} \end{pmatrix} \mathbf{P} \begin{pmatrix} \hat{r}_{k,i} - r_{k,i} \\ \hat{\theta}_{k,i} - \theta_{k,i} \end{pmatrix} > \alpha, \\ 0 & \text{otherwise}, \end{cases} \tag{52}$$

where $\hat{r}_{k,i} = \sqrt{\hat{x}_{k,i}^2 + \hat{y}_{k,i}^2}$, $\hat{\theta}_{k,i} = \arctan\left(\frac{\hat{y}_{k,i}}{\hat{x}_{k,i}}\right)$, $\mathbf{P} = \begin{pmatrix} \frac{1}{\Delta_r} & 0 \\ 0 & \frac{1}{\Delta_\theta} \end{pmatrix}$ and $\alpha = 5.99$ is the value of the quantile function of the chi-square distribution with two degrees of freedom evaluated at 0.95. In other words, at each iteration, we check if the position estimator for each target is located within the 0.95% confidence ellipse around the true target position. Finally, a track is declared to be lost if at least one of the variables $l_{k,i}$ equals 1 during at least five consecutive iterations. We define by f_m the loss variable for the m^{th} Monte-Carlo run that takes value 1 if the filter failed to track the two targets during all the experiment and 0, otherwise. Then, the probability of track loss is given by $\hat{P}_{loss} = \dfrac{1}{N_{MC}} \displaystyle\sum_{m=1}^{N_{MC}} f_m$.

4) Calculation of the Root Mean Square Error (RMSE): The mean RMSE of the two targets is estimated from N_{MC} Monte-Carlo runs with the following procedure: at each iteration, we obtain an estimator of the target state for each target provided by

$$\hat{\mathbf{x}}_{k,i} = \frac{1}{N_p} \sum_{p=1}^{N_p} \mathbf{x}_{k,i}^p, \ i \in \{1, 2\},$$

and we associate each estimator to a target such that the sum of the Euclidean distances between the estimates and the actual state is minimum. Finally, the RMSE is computed at each iteration k for simulations where both targets have not been declared lost (*i.e.* $l_{k,1} = 0$ and $l_{k,2} = 0$) by taking the mean RMSE of the two targets over these simulations.

5) Simulations: The particle filter is performed with the following parameters: $T = 1\,\text{s}$, $q_s = 10^{-3}$, $\sigma_r^2 = 3.6 \times 10^{-3}$, $\sigma_\theta^2 = 1.022 \times 10^{-4}$, $\sigma_v^2 = 0.01$ and $\sigma_n^2 = 0.1$. Parameters for the simulation of the radar measurements are the same as for the monotarget simulation, except for the radar window for which we take $r_{min} = 100\,\text{km}$, $r_{max} = 150\,\text{km}$, $\theta_{min} = -20°$ and $\theta_{min} = +20°$.

Then, as for the monotarget case, performance is evaluated for the three different filters CSM, NCSM and CM already defined, a fourth filter is also used and denoted by ESM (Expectation Squared Modulus) and corresponds to the case where the expectation of the non-centrality parameter is taken to compute the likelihood. Note that for the *Swerling* 0 case there is no interest of using NCSM since CSM requires integration only over $N_k - 1$ phases, therefore we replace the SMNC filter by the LC (for Laplace Coherent), where the likelihood is calculated via its Laplace approximation (see IV-A1).

When the particle states $\mathbf{x}_{k,1}^p$ and $\mathbf{x}_{k,2}^p$ are well separated, the likelihoods are calculated in closed-form according to the corresponding monotarget likelihood expression. When particle states are too close to each other to be assumed disjoint, the likelihoods are computed according to the multitarget likelihood expressions. When this computation requires a numerical integration, this integration is done over 10 points for each parameter. This small number of integration points is explained by the overall computational cost induced when several parameter dimensions are involved.

a) Estimation performance: the performance in terms of RMSE in position and velocity is presented in figures 6, 7 and 8 for the *Swerling* 0, 1 and 3 models respectively. First we observe that in all cases, CM provides the best performance. Then, the difference between the CSM and NCSM is quite small so that it does not seem relevant to take into account the spatial coherence of parameters $\rho_{k,1:N_k}$ and $\varphi_{k,1:N_k}$ with squared modulus. An other important point is to compare the computational time with respect to performance. Thus, in *Swerling* 0 the CL filter is approximatively six times faster than CM filter with almost the same performance. Likewise, in *Swerling* 1 and *Swerling* 3, the NCSM filters are approximatively 60 times faster than CSM. Finally, note that the RMSE in velocity increases when targets are close. This can be explained by the fact that the likelihood does not depend directly on the velocity.

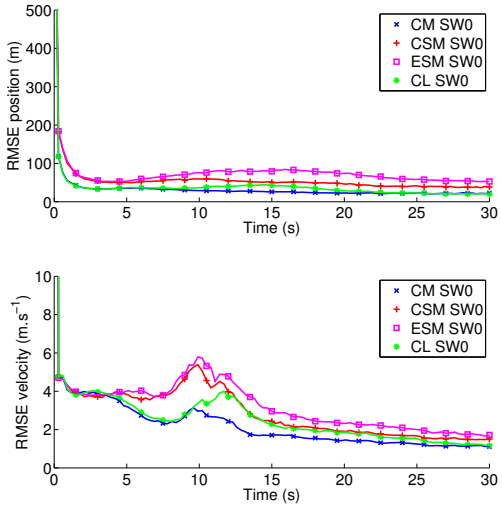

Fig. 6. Monte-Carlo simulation results in a multi-target setting with the *Swerling* 0 model. Top: RMSE in position. Bottom: RMSE in velocity.

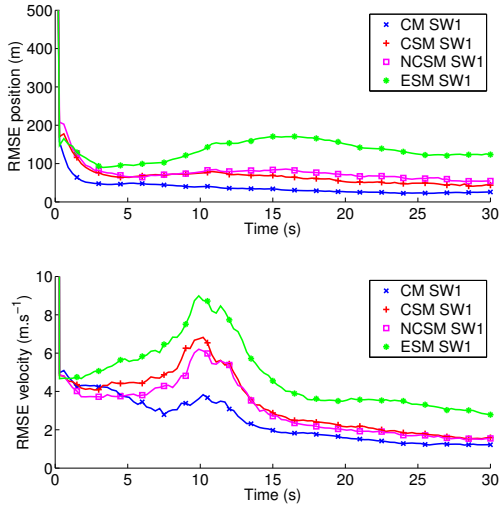

Fig. 7. Monte-Carlo simulation results in a multi-target setting with the *Swerling* 1 model. Top: RMSE in position. Bottom: RMSE in velocity.

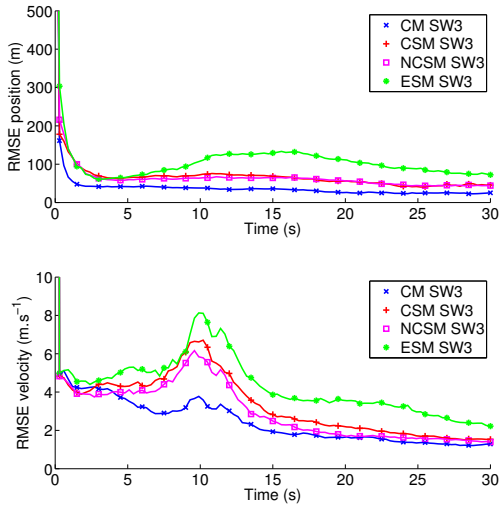

Fig. 8. Monte-Carlo simulation results in a multi-target setting with the *Swerling* 3 model. Top: RMSE in position. Bottom: RMSE in velocity.

b) Track loss performance: We present in Table I, II and III the probability of track loss for fluctuations of type *Swerling* 0, 1 and 3 respectively.

For all the *Swerling* models, the track-loss is minimum for the complex measurement, but filter CSM and NCSM are relatively close to it. The poorest performance is obtained with the ESM filter where the likelihood is computed with a rough approximation but has the advantage to be much more faster than CSM and NCSM.

	Probability of track loss
CM SW0	1.5×10^{-2}
CSM SW0	1.4×10^{-2}
ESM SW0	1.6×10^{-2}
IS SW0	9×10^{-2}

TABLE I

ESTIMATED PROBABILITY OF TRACK LOSS FOR THE DIFFERENT MULTITARGET PARTICLE FILTERS WITH *Swerling* 0 FLUCTUATIONS.

	Probability of track loss
CM SW1	1.6×10^{-2}
CSM SW1	3.1×10^{-2}
NCSM SW1	4×10^{-2}
ESM SW1	6.9×10^{-2}

TABLE II

ESTIMATED PROBABILITY OF TRACK LOSS FOR THE DIFFERENT MULTITARGET PARTICLE FILTERS WITH *Swerling* 1 FLUCTUATIONS.

VI. CONCLUSION

In this paper, we have investigated different methods for computing the likelihood in a radar Track-Before-Detect context. In practice, the likelihood of the complex measurement depends on the unknown complex amplitude parameters of the targets that must be marginalized. We have shown that closed-form expressions can be obtained in the monotarget case for all the *Swerling* models. In the multitarget case, a closed-form can be obtained only for the *Swerling* 1 case; for the others models, we propose some possible approximations to alleviate the computational time and it may be interesting to investigate other approximations that may lead to faster computational time while preserving acceptable performance. We have also considered the case where the data are the squared modulus of the complex measurements. In that case, no closed-form can be obtained and approximations must be performed. Finally, we have demonstrated via Monte-Carlo simulation the benefits of taking into account the spatial coherence of the complex amplitudes both in detection and in estimation compared methods that works on the square modulus of the complex signal. The main conclusions that can be stated based on this work are the following:

- in a TBD context, complex measurements should be used whenever they are available since it appears that the

	Probability of track loss
CM SW3	1×10^{-2}
CSM SW3	1.9×10^{-2}
NCSM SW3	1.5×10^{-2}
ESM SW3	6×10^{-2}

TABLE III

ESTIMATED PROBABILITY OF TRACK LOSS FOR THE DIFFERENT MULTITARGET PARTICLE FILTERS WITH *Swerling* 3 FLUCTUATIONS.

		Swerling 0	Swerling 1	Swerling 3
Complex measurement	Monotarget	Eq.(10) and [1]	***Eq.(31)***	***Eq.(36), Eq.(37)***
	Multitarget	***Eq.(4), and IV-A1***	***Eq.(27)***	***Eq.(4), Eq.(34)***
Squared modulus	Monotarget, non coherent	Eq.(18) and [16]	Eq.(39) and [16]	Eq.(42), Eq.(41) and [16]
	Multitarget, non coherent	***Eq. (20)***	Eq.(39) and [10]	***Eq. (20) and IV-B2***
	Monotarget, coherent	IV-B1 and [1]	IV-B1 and [1]	IV-B1, and [1]
	Multitarget, coherent	***Eq. (19) and IV-B1***	***Eq.(19) and IV-B1***	***Eq.(19) and IV-B1***

TABLE IV

SUMMARY OF THE LIKELIHOOD COMPUTATION WITH DIFFERENT DATA TYPES (COMPLEX MEASUREMENTS OR SQUARED MODULUS), DIFFERENT SWERLING MODELS (TYPE 0, 1 AND 3) AND DIFFERENT NUMBER OF TARGETS (MONO OR MULTITARGET). THE SQUARED MODULUS MEASUREMENT ARE SPLITTED BETWEEN COHERENT COMPUTATION AND NON COHERENT COMPUTATION. EACH CELL CONTAINS THE REFERENCE OF THE EQUATION IN THIS PAPER THAT PROVIDES THE EXPRESSION FOR THE LIKELIHOOD. WHEN THIS EXPRESSION PREVIOUSLY APPEARED IN THE LITERATURE, THE CITATION OF THE CORRESPONDING PAPER IS PROVIDED AS WELL. CONTRIBUTIONS OF THIS PAPER ARE HIGHLIGHTED IN BOLD AND ITALIC.

phases information is very important to improve the performance.

- Multitarget likelihood are not simple to compute except for the particular *Swerling* 1 case. Thus monotarget likelihood should be performed whenever it is possible to factorize the overall joint density.

REFERENCES

[1] S.J. Davey, M.G. Rutten, and B. Cheung. Using phase to improve track-before-detect. *IEEE Transactions on Aerospace and Electronic Systems*, 48(1):832 –849, Jan. 2012.

[2] A. Doucet, S. Godsill, and C. Andrieu. On sequential Monte Carlo sampling methods for Bayesian filtering. *Statistics and Computing*, 10(3):197–208, July 2000.

[3] S.S. Blackman. Multiple hypothesis tracking for multiple target tracking. *Aerospace and Electronic Systems Magazine, IEEE*, 19(1):5–18, Jan 2004.

[4] D.B. Reid. An algorithm for tracking multiple targets. *Automatic Control, IEEE Transactions on*, 24(6):843–854, Dec 1979.

[5] S.S. Blackman. *Multiple-target tracking with radar applications*. Artech House radar library. Norwood, Mass. Artech House, 1986.

[6] T.E. Fortmann, Y. Bar-Shalom, and M. Scheffe. Sonar tracking of multiple targets using joint probabilistic data association. *IEEE Journal of Oceanic Engineering*, 8(3):173–184, 1983.

[7] Y. Bar-Shalom, F. Daum, and J. Huang. The probabilistic data association filter. *Control Systems, IEEE*, 29(6):82–100, Dec 2009.

[8] D.J. Salmond and H. Birch. A particle filter for track-before-detect. In *Proc. American Control Conf.*, pages 3755–3760, 2001.

[9] C. Kreucher, K. Kastella, and A.O. Hero. Multitarget Tracking using the Joint Multitarget Probability Density. *IEEE Trans. on Aerospace and Electronic Systems*, 41(4):1396–1414, 2005.

[10] Y. Boers and J.N. Driessen. Multitarget particle filter track-before-detect application. In *IEE Proc. Radar Sonar Navig.*, volume 151, pages 351–357, 2004.

[11] M.S. Arulampalam, S. Maskell, N. Gordon, and T. Clapp. A tutorial on particle filters for online nonlinear/non-Gaussian Bayesian tracking. *IEEE Transactions on Signal Processing*, 50(2):174 –188, Feb. 2002.

[12] B. Ristic, S. Arulampalam, and N. Gordon. *Beyond the Kalman filter. Particle filters for tracking applications*. Artech House, 2004.

[13] M.I. Skolnik. *Introduction to Radar Systems /2nd Edition/*. McGraw Hill Book Co., New York, 2 edition, 1980.

[14] M.G. Rutten, N.J. Gordon, and S. Maskell. Recursive track-before-detect with target amplitude fluctuations. *IEE Proceedings -Radar, Sonar and Navigation,*, 152(5):345 – 352, Oct. 2005.

[15] S.J. Davey, M.G. Rutten, B. Cheung, and B. Cheung. A comparison of detection performance for several track-before-detect algorithms. In *Information Fusion, 2008 11th International Conference on*, pages 1–8, June 2008.

[16] M. McDonald and B. Balaji. Track-before-detect using Swerling 0, 1, and 3 target models for small manoeuvring maritime targets. *EURASIP J. Adv. Sig. Proc.*, 2008, 2008.

[17] O. Rabaste, C. Riché, and A. Lepoutre. Long-time coherent integration for low SNR target via particle filter in track-before-detect. In *Proceedings of the 15th International Conference on Information Fusion, Singapore 2012*, pages 127–134, Singapore, Singapour, 2012. ISIF.

[18] B.N Vo, B.T. Vo, N.T Pham, and D. Suter. Joint detection and estimation of multiple objects from image observations. *Signal Processing, IEEE Transactions on*, 58(10):5129–5141, 2010.

[19] R.K. Mallik. On multivariate Rayleigh and exponential distributions. *Information Theory, IEEE Transactions on*, 49(6):1499–1515, June 2003.

[20] F.J. Harris. On the use of windows for harmonic analysis with the discrete Fourier transform. *Proceedings of the IEEE*, 66(1):51–83, Jan. 1978.

[21] C. Andrieu, A. Doucet, S.S. Singh, and V.B. Tadic. Particle methods for change detection, system identification, and control. *Proceedings of the IEEE*, 92(3):423–438, 2004.

[22] C. Musso, P. Bui Quang, and F. Le Gland. Introducing the Laplace approximation in particle filtering. In *Proceedings of the 14th International Conference on Information Fusion 2011*, pages 1–8, July 2011.

[23] K.P. Murphy. *Machine Learning: A Probabilistic Perspective*. Adaptive computation and machine learning series. MIT Press, 2012.

[24] M.A. Richards. Relationship between the gamma, Erlang, chi-square, and Swerling 3/4 probability density functions. http://users.ece.gatech.edu/mrichard/Gamma,%20Erlang,%20&%20Chi-Square.pdf, Aug. 2007.

[25] I. S. Gradshteyn and I. M. Ryzhik. *Table of integrals, series, and products*. Elsevier/Academic Press, Amsterdam, seventh edition, 2007.

[26] N. Levanon and E. Mozeson. *Radar signals*. John Wiley and Sons, 2004.

[27] H.L. Van Trees. *Optimum Array Processing, Part IV of Detection, Estimation, and Modulation Theory*. John Wiley and Sons, 2002.

[28] A. Lepoutre, O. Rabaste, and F. Le Gland. Optimized instrumental density for particle filter in track-before-detect. In *9th IET Data Fusion & Target Tracking Conference*, 2012.